Electronic Supplementary Information (ESI)

Regulating Excitonic Effects in Non-Oxide Based $XPSe_3$ (X=Cd, Zn) Monolayers towards Enhanced Photocatalysis for Overall Water Splitting

Amal Kishore[1], Harshita Seksaria[1], Anu Arora, Abir De Sarkar*

Institute of Nano Science and Technology, Knowledge City, Sector 81, Manauli, Mohali, Punjab 140306, India

[1]Both the authors have contributed equally

Email: abir@inst.ac.in, abirdesarkar@gmail.com

Contents

Calculation Details

1.1. Photocatalysis

Step	Reaction Mechanism of OER
R1	$H_2O + * \rightarrow OH^* + e^- + H^+$
R2	$OH^* \rightarrow O^* + e^- + H^+$

R3	$H_2O + O^* \rightarrow HOO^* + e^- + H^+$
R4	$HOO^* \rightarrow * + O_2 + e^- + H^+$

Step	Reaction Mechanism of HER
S1	$H^+ + e^- \rightarrow H^*$
S2	$H^* + H^+ + e^- \rightarrow H_2$

$$\Delta E_{OH} = E_{OH}^* + \frac{1}{2}E_{H_2} - E^* - E_{H_2O}$$

$$\Delta E_O = E_O^* + \frac{1}{2}E_{H_2} - (E_{OH}^* - \Delta E_{OH})$$

$$\Delta E_{OOH} = E_{OOH}^* + \frac{1}{2}E_{H_2} - E_{H_2O} - \left(E_O^* - \Delta E_O\right)$$

Gibbs free energy for these intermediate states, as shown in Table 4, can be calculated by using the following formula:

$$\Delta G = \Delta E + \Delta ZPE - T\Delta S + \Delta G_U + \Delta G_{pH}$$

where ΔE and ΔZPE are the adsorption and zero-point energy per step. $T\Delta S$ is the entropy contribution at T=298K, $\Delta G_U = -eU$ $(e = elementary\ positive\ charge, U = potential\ bias)$. The zero-point energy and the entropic correction in the energy can be determined with the help of vibrational frequencies, as follows:

$$ZPE = \frac{1}{2}\sum h\nu_i$$

$$TS_\nu = k_B T\left[\sum_K ln\left(\frac{1}{1 - e^{-h\nu/k_B T}}\right) + \sum_K \frac{h\nu}{k_B T}\left(\frac{1}{e^{-h\nu/k_B T} - 1}\right) + 1\right]$$

It has been observed that Selenium at the centre of the hexagonal ring happens to be favourable site for the oxygen evolution and the hydrogen evolution reactions. This preference is due to its lowest adsorption energy compared to other sites we have investigated.

Table S1: Characteristics of the reaction sites for OER and HER

System	OER			HER		
	Intermediate	Favourable Site	Adsorber-adsorbate distance (Å)	Intermediate	Favourable Site	Adsorber-adsorbate distance (Å)
$CdPSe_3$	OH	Se	1.6	H^*	Se	1.50
	O	Se	1.72			
	OOH	Se	2.60			
$ZnPSe_3$	OH	Se	1.61	H^*	Se	1.51
	O	Se	1.73			
	OOH	Se	2.62			

Table S2. Calculated adsorption energy ΔE_{ads} and zero-point energy (ΔZPE) of overall reaction step, and Gibbs free energy for the reaction intermediates. All the energies are taken in the units of eV.

System	Reaction Intermediate	ΔE_{ads} (eV)	ΔZPE (eV)	$T\Delta S$ (eV)	Gibbs Free Energy (eV)
$CdPSe_3$	OH^*	3.47	-0.335	-0.011	3.14
	O^*	2.81	-0.456	-0.058	2.41
	OOH*	5.48	-0.310	-0.001	5.17
$ZnPSe_3$	OH^*	3.34	-0.335	-0.011	3.01
	O^*	2.67	-0.456	-0.058	2.27
	OOH*	5.38	-0.310	-0.001	5.07

Table S3. The Gibbs free energy Δ^{G_i} for reaction steps for OER. The sum of Gibbs free energy for the overall mechanism is 4.92 eV, which is the Gibbs free energy for water redox reaction for U=0 eV.

$System$	$\Delta G_1\ (eV)$ **[R1]**	$\Delta G_2(eV)$ **[R2]**	$\Delta G_3\ (eV)$ **[R3]**	$\Delta G_4\ (eV)$ **[R4]**	$\sum_{i=1}^{4} G_i(eV)$
$CdPSe_3$	3.14	-0.73	2.76	-0.25	4.92
$ZnPSe_3$	3.01	-0.74	2.79	-0.15	4.92

Adsorbed geometrical structures and corresponding geometrical changes of $CdPSe_3$ during adsorption of intermediates in water redox reactions:

Further, we have comprehended the major geometrical changes of $CdPSe_3$ and $ZnPSe_3$ with the adsorption of the intermediates. Since the reaction mechanism and absorption kinetics in $CdPSe_3$ and $ZnPSe_3$ are similar, we chose $CdPSe_3$ as the representative model to represent the reaction sequence and the major geometrical changes as shown in Figure S1 and Figure S2 respectively. Interestingly, during the conversion of OH* to O*, the active site 'Se' is a bit distorted from the surface, but it returns to its original state when O* is converted back to OOH*. As a result, the monolayers show no residual geometrical changes, as demonstrated in Figure S2. Upon the release of O_2 (in case of OER), the monolayers return to their exact initial state, illustrating their durability under prolonged and repetitive sequences of reactions. The same has been observed in the case of HER, as can be seen in figure S2 (b).

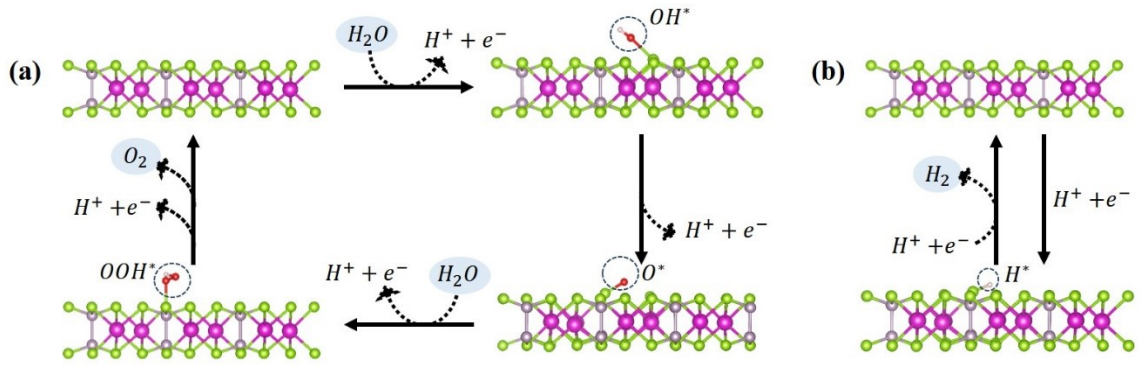

Figure S1: Reaction pathways of (a) oxygen evolution reaction (OER) and (b) hydrogen evolution reaction (HER) half reaction with the most energetically favourable adsorbed

intermediates (OH*, O*, OOH*, and H*) on $CdPSe_3$. The red and rose balls represent oxygen and hydrogen respectively

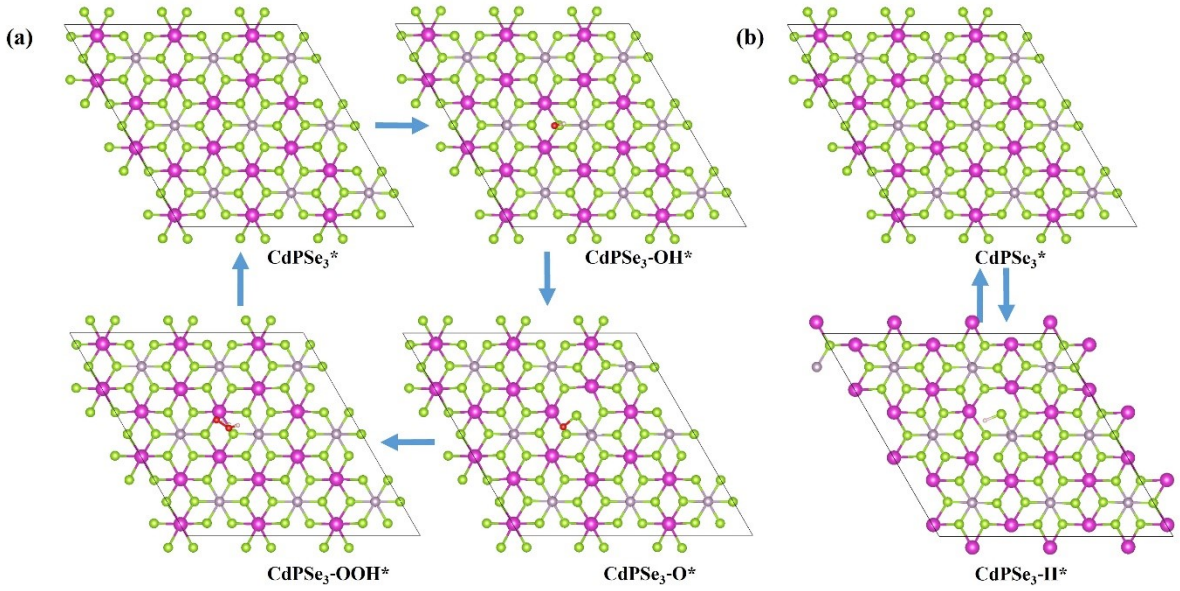

Figure S2. Geometrical changes of $CdPSe_3$ during adsorption of intermediates in (a) OER and (b) HER.

1.2. Exciton Properties

Hamiltonian for an exciton, i.e., interacting electron and hole with anisotropic effective mass, constrained to move in a plane (say x and y plane), is given by

$$\hat{H}_0 = \frac{-\hbar^2}{2}\left(\frac{1}{m_e^x}\frac{\partial^2}{\partial x_e^2} + \frac{1}{m_e^y}\frac{\partial^2}{\partial y_e^2} + \frac{1}{m_h^x}\frac{\partial^2}{\partial x_h^2} + \frac{1}{m_h^y}\frac{\partial^2}{\partial y_h^2}\right) + V(r_e - r_h)$$

where the m_i^j, $j = x, y$, $i = e, h$ corresponds to effective mass of the electron or hole in the x or y direction, respectively; $r_i = (x_i, y_i, z_i)$ describes the positions of electron and hole and V (r_e - r_h) describes the electrostatic interaction between electron and hole.

The Schrödinger equation for the relative motion of electron-hole system is given by

$$\left[-\frac{\hbar^2}{2\mu^x}\frac{\partial^2}{\partial x^2} - \frac{\hbar^2}{2\mu^y}\frac{\partial^2}{\partial y^2} + V(r)\right]\psi(r) = E\psi(r)$$

Where $\mu_x = \frac{m_x^e m_x^h}{m_x^e + m_x^h}$ and $\mu_y = \frac{m_y^e m_y^h}{m_y^e + m_y^h}$ are reduced mass of the exciton in the x and y direction and E and ψ (r) are the eigenenergies and eigenfunctions of the excitons, respectively.

In 2D dielectric medium, electrostatic interaction between electron and hole is given by

$$V_{RK}(r) \equiv V_{RK}(r) = -\frac{\pi k e^2}{2\kappa\rho_0}\left[H_0\left(\frac{r}{\rho_0}\right) - Y_0\left(\frac{r}{\rho_0}\right)\right]$$

Where H_0 and Y_0 are Struve and Bessel functions, respectively.

The 2D polarizability can be calculated using the ab-initio calculated value of the dielectric constant as follows:

$$\epsilon(L) = 1 + \frac{4\pi\chi}{L}$$

$$r_0 = 2\pi\chi$$

r_0 describes the screening length, below which a log(r) interaction dominates while beyond r_0 Coulombic interaction 1/r dominates. It is related to the polarizability as given above.

Employing the variational approach,[1] one finds λ dependent (variational parameter) exciton binding energy $E_x(\lambda)$ and $E_y(\lambda)$ along x and y direction, respectively. λ is the variational anisotropy scaling factor relating the spatial extent of exciton along x direction, a_x, and one along a_y along the y direction, $a_y = \lambda a_x$.

$$E_{x(y)}(\lambda) = \frac{e^2}{4\pi\varepsilon_0\epsilon r_0}\left\{\frac{3}{2} + ln\left(\frac{\tilde{a_{x(y)}}(\lambda)\lambda + 1}{4r_0}\right)\right\}$$

$$\tilde{a}_x(\lambda) = \sqrt{a_0 r_0 \frac{\epsilon m}{\mu_{xy}(\lambda)}}$$

$$\tilde{a}_y(\lambda) = \lambda\tilde{a}_x(\lambda)$$

$$\mu_{x(y)} = \frac{m_{x(y)}^e m_{x(y)}^h}{m_x^e + m_x^h}$$

$$\mu_{xy}(\lambda) = 2\left(\frac{1}{\mu_x} + \frac{1}{\lambda^2 \mu_y}\right)^{-1}$$

$$\lambda = \left(\frac{\mu_x}{\mu_y}\right)^{\frac{1}{3}}$$

Phonon Band Structure

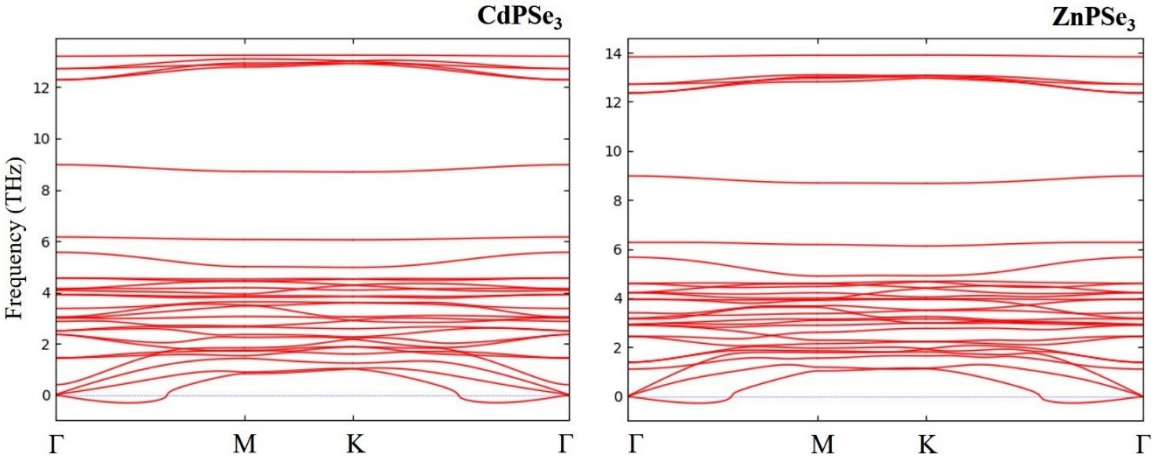

Figure S3. Phonon Dispersion of $CdPSe_3$ and $ZnPSe_3$ monolayers

The phonon spectrum was calculated using the PHONOPY code.[2] The absence of imaginary frequency except a small amount of negative frequency near the Γ point which is less than 10 cm^{-1} or 0.3 THz which is acceptable shows the dynamical stability.[3,4] This negative frequency is often a result of numerical artifacts and can be eliminated by increasing the density of the K-mesh and using a larger supercell.[5,6] Moreover, as mentioned in the manuscript, these monolayers are already synthesized.[7,8]

Elastic Stiffness

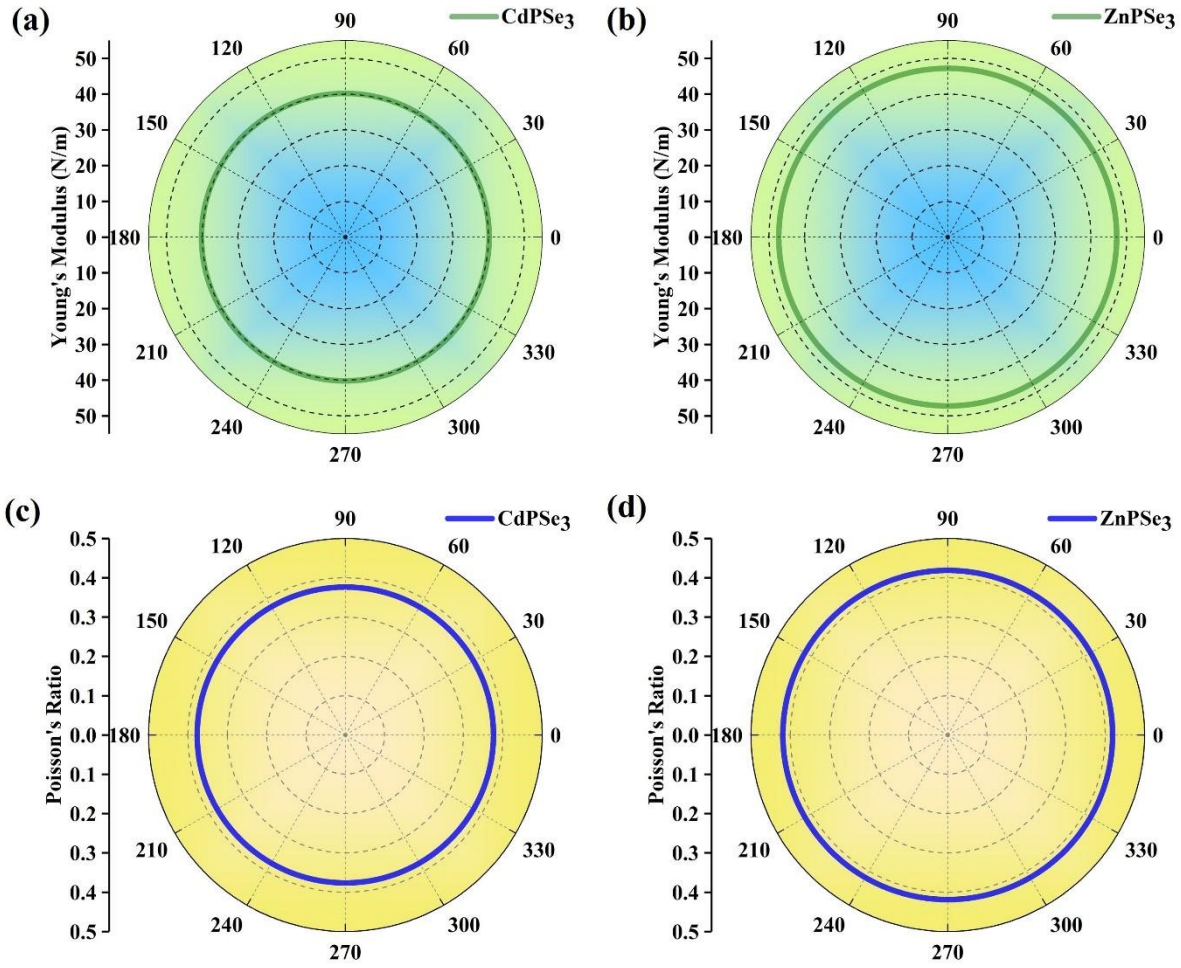

Figure S4. (a, c) Young's modulus Y(θ), (b, d) Poisson's ratio ν(θ) of monolayers $CdPSe_3$ and $ZnPSe_3$ as a function of θ. Here, θ = 0° and θ = 90° indicate x- and y-directions, respectively.

Table S4. Elastic Stiffness coefficients, Young's modulus and Poisson's ratio for $CdPSe_3$ and $ZnPSe_3$

Systems	$C_{11} = C_{22}$ (N/m)	$C_{12} = C_{21}$ (N/m)	C_{66} (N/m)	Young's Modulus (N/m)	Poisson's Ratio
$CdPSe_3$	46.55	17.49	14.53	39.98	0.37
$ZnPSe_3$	58.39	23.28	17.55	49.11	0.40

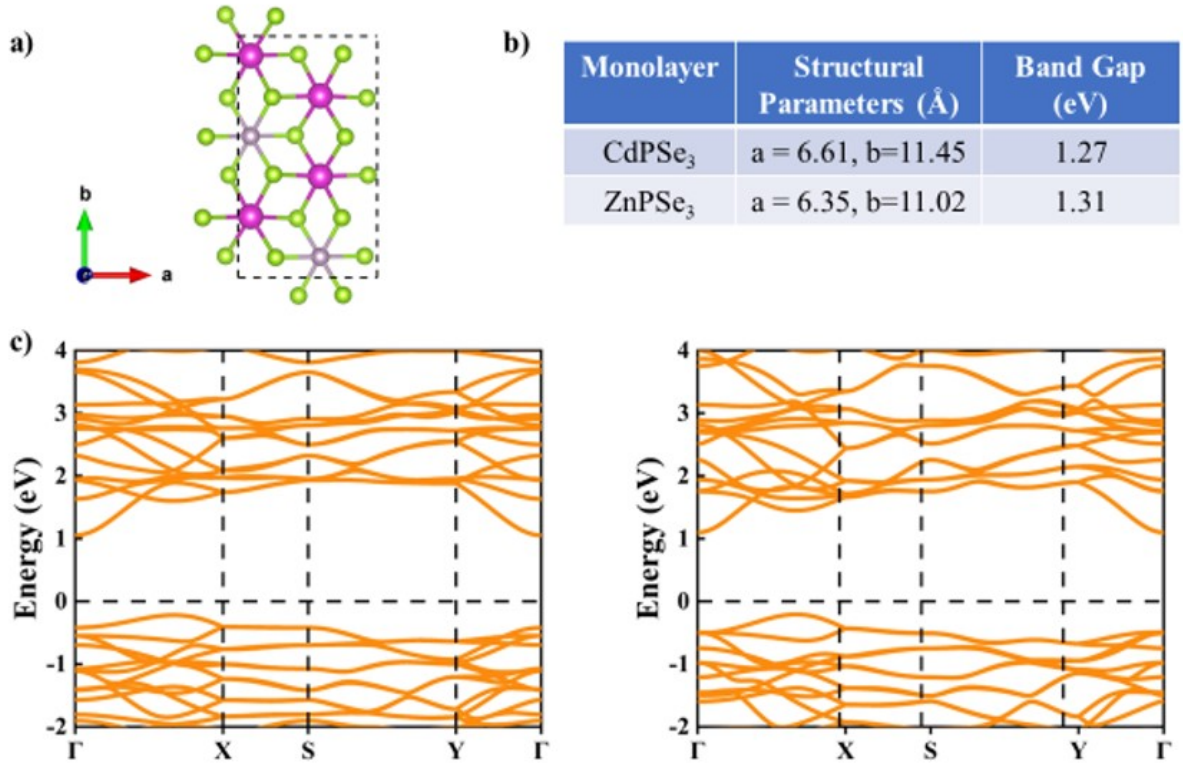

Figure S5. (a) Orthogonal unit cell (b) lattice parameters and band gap (c) band structure of $cdPSe_3$ and (d) band structure of $ZnPSe_3$

Exciton Binding Energy vs Bohr Radius Plot

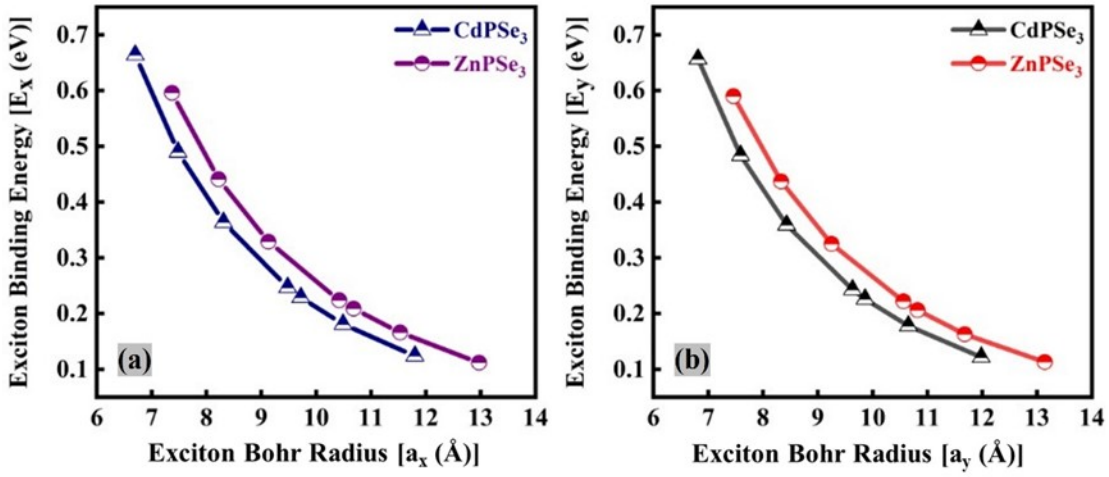

Figure S6. Exciton binding energy as a function of exciton Bohr radius along x and y directions

References:

1 E. Prada, J. V. Alvarez, K. L. Narasimha-Acharya, F. J. Bailen and J. J. Palacios, Effective-mass theory for the anisotropic exciton in two-dimensional crystals: Application to phosphorene, *Phys Rev B*, 2015, **91**, 245421.

2 A. Togo and I. Tanaka, First principles phonon calculations in materials science, *Scr Mater*, 2015, **108**, 1–5.

3 R. Peng, Y. Ma, Z. He, B. Huang, L. Kou and Y. Dai, Single-Layer Ag_2S: A Two-Dimensional Bidirectional Auxetic Semiconductor, *Nano Lett*, 2019, **19**, 1227–1233.

4 J. Zhou, J. Huang, B. G. Sumpter, P. R. C. Kent, Y. Xie, H. Terrones and S. C. Smith, Theoretical Predictions of Freestanding Honeycomb Sheets of Cadmium Chalcogenides, *The Journal of Physical Chemistry C*, 2014, **118**, 16236–16245.

5 H. Şahin, S. Cahangirov, M. Topsakal, E. Bekaroglu, E. Akturk, R. T. Senger and S. Ciraci, Monolayer honeycomb structures of group-IV elements and III-V binary compounds: First-principles calculations, *Phys Rev B*, 2009, **80**, 155453.

6 S. Cahangirov, M. Topsakal, E. Aktürk, H. Şahin and S. Ciraci, Two- and One-Dimensional Honeycomb Structures of Silicon and Germanium, *Phys Rev Lett*, 2009, **102**, 236804.

7 J. Zhou, C. Zhu, Y. Zhou, J. Dong, P. Li, Z. Zhang, Z. Wang, Y.-C. Lin, J. Shi, R. Zhang, Y. Zheng, H. Yu, B. Tang, F. Liu, L. Wang, L. Liu, G.-B. Liu, W. Hu, Y. Gao, H. Yang, W. Gao, L. Lu, Y. Wang, K. Suenaga, G. Liu, F. Ding, Y. Yao and Z. Liu, Composition and phase engineering of metal chalcogenides and phosphorous chalcogenides, *Nat Mater*, , DOI:10.1038/s41563-022-01291-5.

8 M. Grzeszczyk, K. S. Novoselov and M. Koperski, $ZnPSe_3$ as ultrabright indirect band-gap system with microsecond excitonic lifetimes, *Proceedings of the National Academy of Sciences*, , DOI:10.1073/pnas.2207074119.